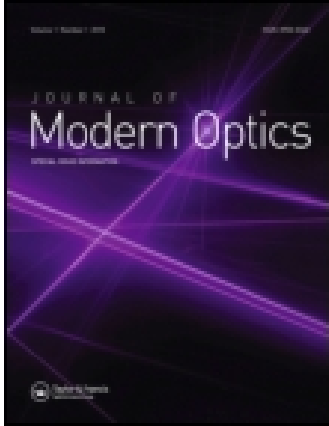


This article was downloaded by: [Fernando Perez Quintian]

On: 04 May 2015, At: 06:15

Publisher: Taylor & Francis

Informa Ltd Registered in England and Wales Registered Number: 1072954 Registered office: Mortimer House, 37-41 Mortimer Street, London W1T 3JH, UK



## Journal of Modern Optics

Publication details, including instructions for authors and subscription information:

<http://www.tandfonline.com/loi/tmop20>

### Ultrasonic Lamb waves detection using an unstabilized optical interferometer with uncalibrated phase shifts

Natalia Alvarez<sup>a</sup>, María Teresa Garea<sup>a</sup> & Fernando Perez Quintián<sup>bc</sup>

<sup>a</sup> Facultad de Ingeniería, Departamento de Física, Universidad de Buenos Aires, Argentina.

<sup>b</sup> Facultad de Ingeniería, Departamento de Física, Universidad Nacional del Comahue, Neuquén, Argentina.

<sup>c</sup> CONICET, Buenos Aires, Argentina.

Published online: 14 Jan 2015.



[Click for updates](#)

To cite this article: Natalia Alvarez, María Teresa Garea & Fernando Perez Quintián (2015) Ultrasonic Lamb waves detection using an unstabilized optical interferometer with uncalibrated phase shifts, *Journal of Modern Optics*, 62:7, 556-559, DOI: [10.1080/09500340.2014.992991](https://doi.org/10.1080/09500340.2014.992991)

To link to this article: <http://dx.doi.org/10.1080/09500340.2014.992991>

PLEASE SCROLL DOWN FOR ARTICLE

Taylor & Francis makes every effort to ensure the accuracy of all the information (the "Content") contained in the publications on our platform. However, Taylor & Francis, our agents, and our licensors make no representations or warranties whatsoever as to the accuracy, completeness, or suitability for any purpose of the Content. Any opinions and views expressed in this publication are the opinions and views of the authors, and are not the views of or endorsed by Taylor & Francis. The accuracy of the Content should not be relied upon and should be independently verified with primary sources of information. Taylor and Francis shall not be liable for any losses, actions, claims, proceedings, demands, costs, expenses, damages, and other liabilities whatsoever or howsoever caused arising directly or indirectly in connection with, in relation to or arising out of the use of the Content.

This article may be used for research, teaching, and private study purposes. Any substantial or systematic reproduction, redistribution, reselling, loan, sub-licensing, systematic supply, or distribution in any form to anyone is expressly forbidden. Terms & Conditions of access and use can be found at <http://www.tandfonline.com/page/terms-and-conditions>

## Ultrasonic Lamb waves detection using an unstabilized optical interferometer with uncalibrated phase shifts

Natalia Alvarez<sup>a\*</sup>, María Teresa Garea<sup>a</sup> and Fernando Perez Quintián<sup>b,c</sup>

<sup>a</sup>Facultad de Ingeniería, Departamento de Física, Universidad de Buenos Aires, Argentina; <sup>b</sup>Facultad de Ingeniería, Departamento de Física, Universidad Nacional del Comahue, Neuquén, Argentina; <sup>c</sup>CONICET, Buenos Aires, Argentina

(Received 6 October 2014; accepted 25 November 2014)

We present an experimental and post-processing scheme that allows ultrasound surface wave detection by means of an unstabilized homodyne interferometric technique. We register interference signals for a set of uncalibrated phase shifts and, from them, we are able to retrieve the normal surface displacement of a thin aluminium plate. The results obtained with this technique are then compared to robust and more traditional phase recovery methods such as the Carré algorithm and the 11-step windowed discrete Fourier transform algorithm. For both algorithms, we found a correlation superior to 99.9%, when compared to the results of the proposed technique. This non-destructive testing scheme represents a simpler and less-expensive alternative to other existing laser ultrasonic techniques.

**Keywords:** phase shift; phase retrieval; interferometry; surface waves; non-destructive testing; laser ultrasonics

### 1. Introduction

Ultrasound techniques have been used in non-destructive testing and process control to successfully determine material properties and structural features for some decades now [1–3]. Nevertheless, it is still a very active field of investigation and widely used in the inspection of materials, characterization and damage detection [4–7].

Conventional ultrasonic techniques use piezoelectric transducers for generation and detection of the surface waves, but they have limitations, such as the need of contact between the sample and the transducers, usually require the use of a couplant and have a limited detection bandwidth [8]. Another alternative available is to employ electromagnetic acoustic transducers (EMATs) [9]. These transducers consist of a magnet and an electric coil and are able to generate and detect acoustic waves within the material with two interaction mechanisms: Lorentz force and magnetostriction. This technique eliminates the necessity of a couplant and does not require physical contact with the test sample. However, proximity to the sample is still needed and it is limited to metallic or magnetic samples. The size of the EMAT transducers is another limiting factor.

These previously mentioned limitations are eliminated by the laser ultrasonics technique [10], which uses lasers for both the generation and detection of the ultrasound. This is a very versatile remote technique, making it suitable for use in hostile environments. There are several optical methods that allow detecting surface ultrasound waves, which have

typically an amplitude of a few nanometres. Most of them involve the phase measurement, achieved by measuring the coherent interference between a reference and a sample beam. In heterodyne interferometry, the reference and sample beams have slightly different frequencies, so the information about the sample displacement is encoded in the beat signal and is usually electronically processed to recover it. In homodyne detection, both beams have the same frequency and the surface displacement, consisting typically of a few nanometres, is quantitatively recovered by retrieving the phase from the registered interference pattern.

Many different techniques for quantitative phase retrieval from interference patterns have been developed in the last decades [11–14]. To recover the phase from the interference signal, phase shifts are usually introduced during the measurement, which need to be precisely calibrated. Mechanical vibration, air turbulence and other environmental conditions affect the phase shifts causing errors during the phase retrieval process. It is important to note that the phase variation generated by nanometric surface displacements is usually much smaller than the phase variation caused by vibrations. Some of this undesirable noise can be minimized by introducing an active phase feedback circuit in the reference beam which stabilizes the interferometer with, for example, a mechanical positioner such as a PZT, acousto-optic or electro-optic modulation [10,15–17]. A much more simple approach consists of using the vibrations present in the system as a source of random phase shifts. Hao et al. [18]

\*Corresponding author. Email: [nalvarez@fi.uba.ar](mailto:nalvarez@fi.uba.ar)

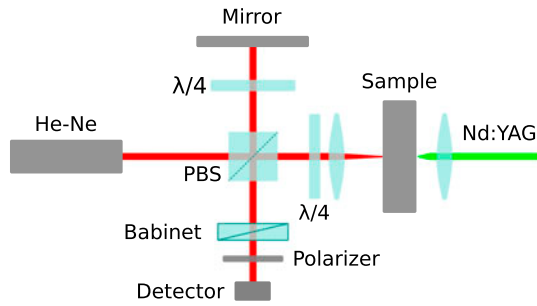


Figure 1. Experimental set-up. (The colour version of this figure is included in the online version of the journal.)

proposed a technique with random phase shifts to recover the spatial distribution of the phase in two-dimensional images. In the following sections, we show how to successfully apply an equivalent mechanism in order to recover the temporal phase distribution from ultrasound signals.

## 2. Experimental arrangement

The experimental set-up that allows the generation and detection of ultrasound is shown in Figure 1. The detection is done using an unstabilized polarizing Michelson interferometer. This arrangement has several advantages over other interferometers, besides its simplicity. On the one hand, the use of a polarizing beam splitter with quarter-wave plates and a linearly polarized laser maximizes the use of the available light power, since all the light is directed to the detector. This also avoids feedback to the laser, which can be a source of instability. On the other hand, this set-up reduces sensitivity to noise since the beam is focused onto the surface. This makes the signal much less sensitive to the tilting of the surface and also enables good performance to be achieved with surfaces not having a good optical finish.

The signal and the reference beams are orthogonally polarized after recombining in the beam splitter. A Babinet compensator in the output beam allows to introduce a global phase difference between the signal and the reference, which can take any value between 0 and  $4\pi$ . The polarizer is used to obtain interference between the orthogonal components.

As an example of the applicability of the technique, we detected ultrasound waves on aluminium plates with 0.5 mm of thickness. The experimental method consisted of impinging on the sample with a focused Nd:YAG pulsed laser line to generate ultrasonic Lamb waves in the thermoelastic regime. Surface waves were detected, 20 mm off the epicenter, with the homodyne interferometer for different values of retardation introduced by the Babinet compensator.

## 3. Uncalibrated phase shifts technique

When the Nd:YAG laser pulse illuminates the sample, an ultrasonic wave is generated. Surface waves are detected

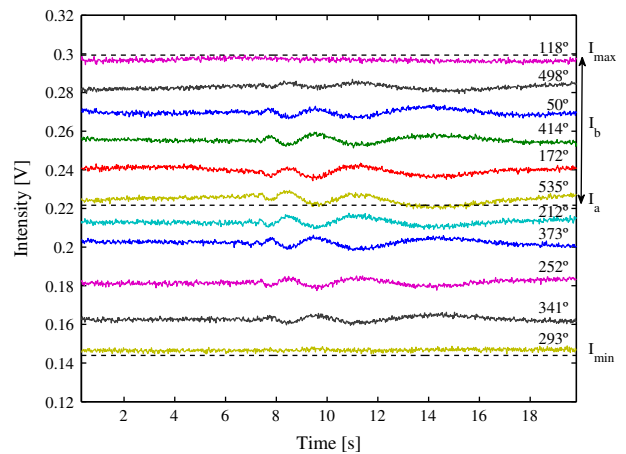


Figure 2. Interference signals registered for different Babinet retardations, which are indicated in degrees for each signal. (The colour version of this figure is included in the online version of the journal.)

by the interferometer and its output is digitally registered. We then modify the retardation introduced by the Babinet compensator and we repeat another measurement. After repeating this process  $M = 400$  times, monotonically varying the Babinet retardation in the interval  $[0, 4\pi]$ , we obtain different interferogram signals. As an example, some of these signals have been plotted in Figure 2.

The signal registered by the detector for the  $i$ th interferogram will be:

$$I(t, i) = I_a + I_b \cos[\Delta\phi(t) + \varphi(t, i)] \quad (1)$$

where  $\Delta\phi(t)$  corresponds to the phase originated by the ultrasound and  $\varphi(t, i)$  consists of a global phase given by the Babinet compensator  $\varphi_B$  and also by the presence of noise  $\varphi_N$ , such as mechanical vibration, air turbulence and surface tilting during the measurement. All these effects vary slowly compared to the typical ultrasonic frequencies, so it is a good approximation to consider them constant during each measurement.

$$\varphi(t, i) = \varphi_B(i) + \varphi_N(t, i) \approx \varphi_B(i) + \varphi_N(i) = \varphi(i) \quad (2)$$

Since the surface displacement originated by the ultrasound is much smaller than the He-Ne wavelength, the phase fluctuation generated by the ultrasound is small. So, for global phases near  $0, \pi, 2\pi, \dots$ , such that the intensity in (1) approaches its maxima and minima, the fluctuation of the signal generated by the ultrasound practically vanishes in Figure 2. Conversely, for global phase values near  $\pi/2, 3\pi/2, \dots$ , the system acquires its best sensitivity.

The random phase shift technique requires monotonically varying  $\varphi_B$  in an interval of at least  $[0, 2\pi]$ . There is no need for these phase steps to be regularly distributed nor to be accurately controlled. In Figure 3, we show the dependency of the registered intensity at a fixed time as a function

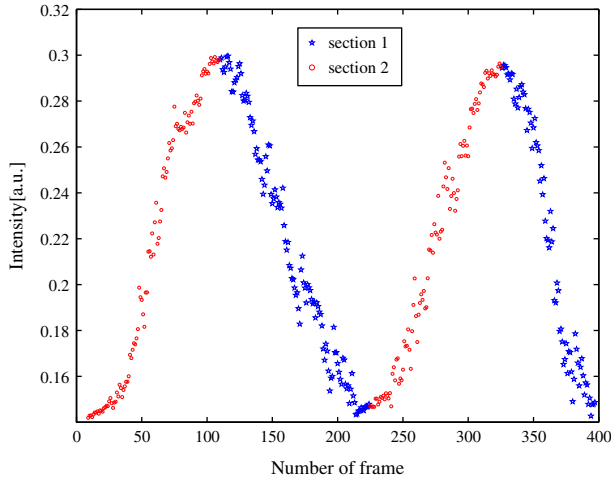


Figure 3. Intensity fluctuation with monotonically varying Babinet phase, obtained at a fixed time for each interferogram. (The colour version of this figure is included in the online version of the journal.)

of the number of phase steps introduced by the Babinet compensator.

Since the global phase sweeps the interval  $[0, 4\pi]$ , maxima and minima are reached in Figure 3. In this plot, we can distinguish the Section 1 (the curve between a maximum and a minimum) and Section 2 (the curve between a minimum and a maximum) introduced by Hao et al. [18] that we will use later. We can also note that the phase difference caused by the noise  $\varphi_N(i)$  can be larger than the phase steps introduced by the Babinet compensator, resulting in a non-monotonically varying overall phase. This does not affect the phase retrieval process at all, as long as we can still identify the maxima and minima that define Sections 1 and 2. This insensitivity to noise makes the technique very robust. We can use the maxima and minima information to autocalibrate the system and obtain a normalized version of the registered voltage signals  $\hat{I}$  by computing  $I_a$  and  $I_b$  in (1) as:

$$\begin{aligned} I_a &= \{\max[I(t, i)] + \min[I(t, i)]\} / 2 \\ I_b &= \{\max[I(t, i)] - \min[I(t, i)]\} / 2 \\ \hat{I}(t, i) &= \frac{I(t, i) - I_a}{I_b} \end{aligned} \quad (3)$$

We can retrieve the complete phase for each interferogram in the interval  $[0, \pi]$  as:

$$\Phi(t, i) = \arccos \left[ \hat{I}(t, i) \right] \quad (4)$$

In order to obtain the phase in the extended interval  $[0, 2\pi]$ , it is necessary to acknowledge that because of the symmetry of the cosine function, the phase values in Section 2 (in Figure 3) will be related to the extended phase by computing  $[2\pi - \Phi(t, i)]$ .

As stated before, the ultrasound phase fluctuations are small enough so that we do not need to apply an unwrapping

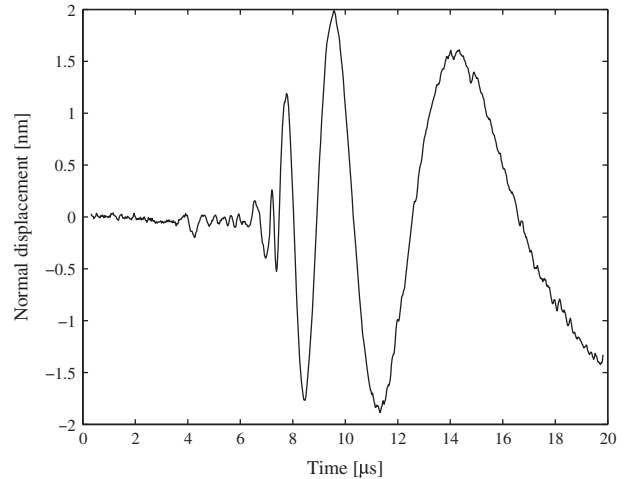


Figure 4. Mean surface displacement.

operator, but it can be applied if phase fluctuations extend beyond the interval  $[0, 2\pi]$ . Finally, we can estimate the original phase  $\Delta\phi(t)$  generated by the ultrasound waves by computing the mean value from all the interferograms. The phase difference is related to the surface displacement by the factor  $\lambda/4\pi$ . In Figure 4, we show the plot obtained with this technique for the mean surface displacement.

#### 4. Comparison with other phase shifting techniques

We compared the random phase shift technique results with the ones obtained from two more traditional techniques: the Carré algorithm [19] and the 11-step windowed discrete Fourier transform (WDFT) phase shifting algorithm [20,21]. These two methods require precise phase stepping values.

The Carré algorithm is one of the most often used algorithms with an arbitrary phase step. It requires four interferograms with an arbitrary but uniform phase stepping  $\alpha$ . Kemao et al. [22] did a study to determine the best suitable phase stepping for the Carré algorithm that minimized both intensity errors and phase shift errors. They found that  $\alpha = 110^\circ$  met these criteria, so we implemented the Carré algorithm using this phase step.

The 11-step WDFT method belongs to a family of phase shifting algorithms designed to present insensitivity to both the harmonic content and the phase shift miscalibration. This method requires 11 interferograms with a fixed phase stepping  $\alpha = 60^\circ$ .

In Figure 5, we show the mean surface displacement of the three different phase recovery techniques for the case of ultrasonic Lamb waves detected 20 mm off the epicentre on an aluminium sample of 0.5 mm of thickness. To quantitatively measure the similarity between the output of the random phase shift method with the four-step Carré and the 11-step WDFT methods, we computed the cross-correlation of each pair of signals, obtaining a maximum value of 99.92

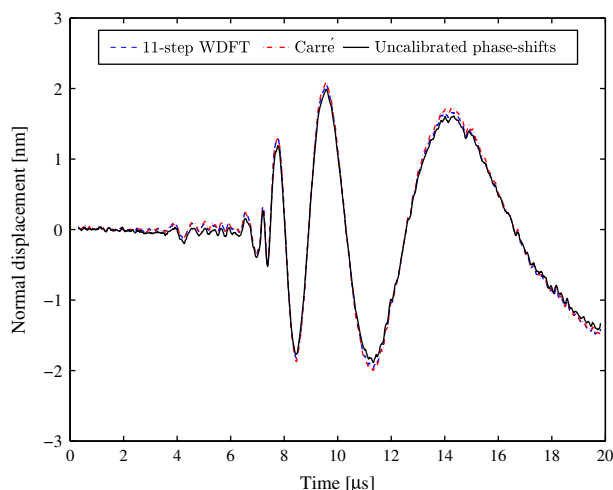


Figure 5. Mean surface displacement for the three different phase recovery techniques. (The colour version of this figure is included in the online version of the journal.)

and 99.93%, respectively. We also obtained a displacement error inferior to 0.14 nm in all cases.

## 5. Conclusions

We successfully detected ultrasonic Lamb waves with an unstabilized homodyne interferometer and were able to retrieve the normal displacement of the sample by applying the uncalibrated phase shift technique to temporal phase measurement. We found that the results from this technique are highly correlated to the results given by traditional methods for phase recovery, which require a calibration of the phase steps.

The presented experimental set-up is very simple, since we do not require stabilization of the interferometer, nor we use quadrature detection involving multiple detectors. This reduces its cost and also facilitates the system alignment.

Considering the fact that we experimentally introduce a phase excursion greater than  $2\pi$ , we are able to trivially relate phase values to surface displacement in each measurement without the need to calibrate our experimental set-up. This autocalibrating feature makes this technique very robust and less error prone.

## Funding

This work was supported by the Universidad de Buenos Aires under [grant number UBACyT (2011–2014) 20020100100139], and [grant number UBACyT (2013–2016) 20020120100025BA]; ANPCYT under [grant number PICT2008-77].

## References

- [1] Beall, F.C. *Wood Sci. Technol.* **2002**, *36*, 197–212.
- [2] D’Orazio, T.; Leo, M.; Distanto, A.; Guaragnella, C.; Pianese, V.; et al. *NDT E Int.* **2008**, *41*, 145–154.
- [3] Awad, T.; Moharram, H.; Shaltout, O.; Asker, D.; et al. *Food Res. Int.* **2012**, *48*, 410–427.
- [4] Martínez-Martínez, J.; Benavente, D.; del Cura, M.G. *Eng. Geol.* **2011**, *119*, 84–95.
- [5] Mutlu, I.; Oktay, E.; Ekinici, S. *Russian J. Nondestr. Test.* **2013**, *49*, 112–120.
- [6] Nunes, T.M.; de Albuquerque, V.H.C.; Papa, J.P.; Silva, C.C.; Normando, P.G.; Moura, E.P.; et al. *Expert Syst. Appl.* **2013**, *40*, 3096–3105.
- [7] Ruiz, A.; Ortiz, N.; Medina, A.; Kim, J.Y.; et al. *NDT E Int.* **2013**, *54*, 19–26.
- [8] Castaings, M.; Hosten, B. *NDT E Int.* **2001**, *34*, 249–258.
- [9] Pei, C.; Fukuchi, T.; Zhu, H.; Koyama, K.; Demachi, K.; et al. *IEEE Trans. Ultrason. Ferroelectrics Freq. Contr.* **2012**, *59*, 2702–2708.
- [10] Scruby, C.B.; Drain, L.E. *Laser Ultrasonics: Techniques and Applications*. Adam Hilger, Bristol, 1990.
- [11] Juárez-Salazar, R.; Robledo-Sánchez, C.; Guerrero-Sánchez, F.; et al. *Opt. Express* **2014**, *22*, 4738–4750.
- [12] Liu, Q.; Wang, Y.; Ji, F.; et al. *Opt. Express* **2013**, *21*, 29505–29515.
- [13] Surrel, Y. *Appl. Opt.* **1996**, *35*, 51–60.
- [14] Takeda, M.; Ina, H.; Kobayashi, S. *J. Opt. Soc. Am.* **1982**, *72*, 156–160.
- [15] Briles, T.C.; Yost, D.C.; Cingöz, A.; Ye, J.; et al. *Opt. Express* **2010**, *18*, 9739–9746.
- [16] Xia, W.; Wang, M.; Yang, Z.; Guo, W.; Hao, H.; et al. *Appl. Opt.* **2013**, *52*, B52–B59.
- [17] Jotzu, G.; Bartley, T.J.; Coldenstrod-Ronge, H.B.; Smith, B.J.; et al. *J. Mod. Optic.* **2012**, *59*, 42–45.
- [18] Hao, Q.; Zhu, Q.; Hu, Y. *Opt. Lett.* **2009**, *34*, 1288–1290.
- [19] Carré, P. *Metrologia* **1966**, *2*, 13–23.
- [20] Hibino, K.; Larkin, K.; Oreb, B.F.; et al. *J. Opt. Soc. Am. A* **1995**, *12*, 761–768.
- [21] Surrel, Y. *Appl. Opt.* **1997**, *36*, 271–276.
- [22] Kemao, Q.; Fangjun, S.; Xiaoping, W. *Meas. Sci. Tech.* **2000**, *11*, 1220–1223.